

X-ray analysis and modeling of the PWN in G0.9+0.1

Markus Holler, Fabian Matthias Schöck, Peter Eger, Dominik Kießling, Kathrin Valerius, Christian Stegmann

ECAP, Erlangen, Germany

The source

The composite supernova remnant (SNR) G0.9+0.1 is located less than one degree from the Galactic Center (GC). The overall radio morphology is dominated by a luminous core with a diameter of $\approx 2'$ surrounded by a fainter, but still well detectable shell with a diameter of $\approx 8'$ (Helfand & Becker 1987). X-ray observations with Chandra (Gaensler et al. 2001) and XMM-Newton (Porquet et al. 2003) unambiguously identified the core of the SNR as a pulsar wind nebula (PWN). Gaensler et al. (2001) found an unresolved source (CXOU J174722.8–280915) approximately $10''$ south of the region of brightest emission (see Fig. 1). Due to the high sensitivity of XMM-Newton, Porquet et al. (2003) were able to detect faint X-ray emission from the shell of the SNR. Dubner et al. (2008) showed that the X-ray PWN almost fills the size of the radio core, which indicates a moderate magnetic field (see e.g. Gaensler & Slane 2006). G0.9+0.1 has been detected with H.E.S.S. (Aharonian et al. 2005) in very high energy (VHE, $E > 100$ GeV) γ -rays above 200 GeV. The source exhibits a flux of only 2 % compared to the one of the Crab Nebula. For H.E.S.S., it appears point-like, with an upper limit on the intrinsic angular extent between $1.3'$ and $2.2'$, depending on the assumed morphology. In 2009, Camilo et al. discovered PSR J1747-2809, the pulsar powering G0.9+0.1. The authors report a strongly scattered and dispersed signal with a pulsation period of $P = 52$ ms. The characteristic age was derived as $\tau_c = 5.3$ kyr and the spin-down luminosity as $dE/dt = 4.3 \times 10^{37}$ erg/s. The high scattering of the signal increases the positional uncertainty to about $3'$, neither proving nor disproving that CXOU J174722.8–280915 is the X-ray counterpart of PSR J1747-2809.

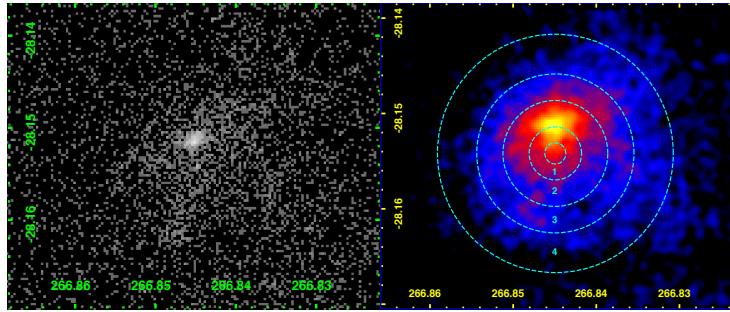


Fig. 1. Chandra count map of the inner part of the PWN containing the point source CXOU J174722.8–280915 south of the region of brightest emission.

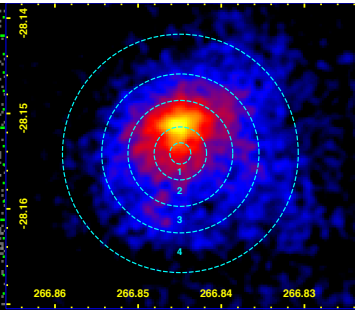


Fig. 2. Smoothed XMM-Newton count map merged from the MOS and pn data of the 2000 and 2003 observations. The annuli are encompassed by dashed cyan lines.

Spectral properties

We analyzed two XMM-Newton on-axis observations (Observation IDs 0112970201 and 0144220101) with 14 respectively 36 ks exposure after background screening. The extracted spectra of the pn and MOS cameras were fitted in parallel with an absorbed power-law model. We used the *tbabs* absorption model, along with the abundances from Wilms et al. (2000). In order to obtain a statistically significant result for the absorption column density, we first fitted the spectrum of a circular region with a radius of $45''$, in the energy range 0.2–10 keV. The circle was centered on CXOU J174722.8–280915, the putative position of PSR J1747-2809. The result is $N_H = (2.26 \pm 0.15) \times 10^{23} \text{ cm}^{-2}$. For the modeling of the emission, we extracted spectra of four annuli centered on the position of CXOU J174722.8–280915, which are illustrated in Fig. 2. The inner and outer radii are $4\text{--}10''$, $10\text{--}20''$, $20\text{--}30''$, and $30\text{--}45''$, respectively. We fixed N_H to $2.26 \times 10^{23} \text{ cm}^{-2}$ for the individual annuli. As an example, Fig. 3 shows the spectrum of the second annulus.

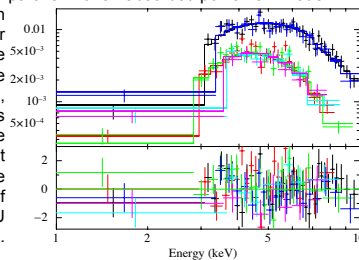


Fig. 3. Energy spectrum extracted from the second annulus. The data were fitted in parallel with an absorbed power-law model.

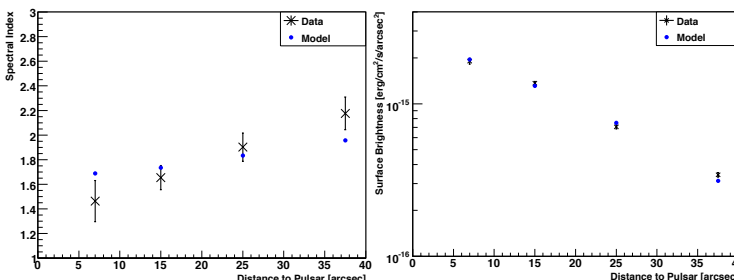
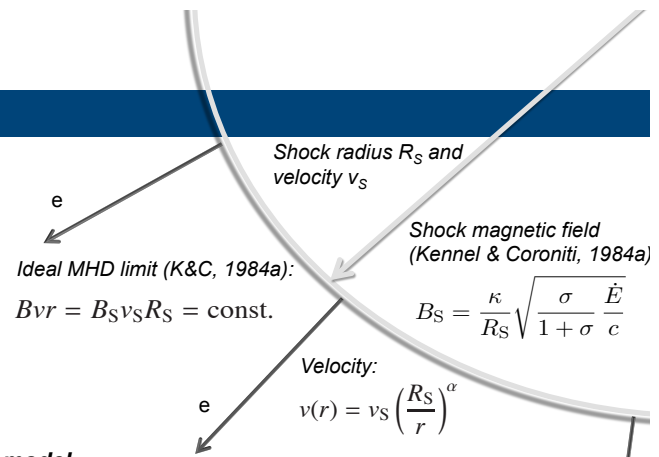


Fig. 4. Evolution of the modeled and measured spectral index (left panel) and surface brightness (right panel) with increasing angular distance to the pulsar.



The model

We assume that the shape of the lepton population which is continuously injected at the termination shock is given by (e.g. Kennel & Coroniti 1984b)

$$Q(E_e) = Q_0 E_e^{-p},$$

with the lepton energy E_e , the spectral index p (which is set to 2 in our case), and the normalization constant Q_0 . The relations that determine the leptonic outflow are given in the sketch above. As the leptons propagate outwards, they lose energy, leading to a change of the spectral shape. Two fundamental energy loss mechanisms have to be considered: synchrotron radiation of the leptons and adiabatic energy losses. They are given by (de Jager & Harding 1992)

$$\frac{dE_e}{dt} = -\frac{E_e}{3} \nabla \cdot \mathbf{v}_l(r) - 2.368 \times 10^{-3} (B E_e)^2 \frac{\text{erg}}{\text{s}}.$$

For a certain set of parameters, we numerically calculated the synchrotron emission of the same annuli as chosen for the XMM-Newton analysis. The parameters were then optimized so that the modeled radiation matches the X-ray data. The results for the evolution of the spectral index and surface brightness are shown in Fig. 4.

Implications for the VHE γ -ray emission

Assuming that the same lepton population that emits synchrotron radiation also scatters photons up to the VHE range, we calculated the inverse Compton (IC) radiation of the whole modeled area for the best parameter set.

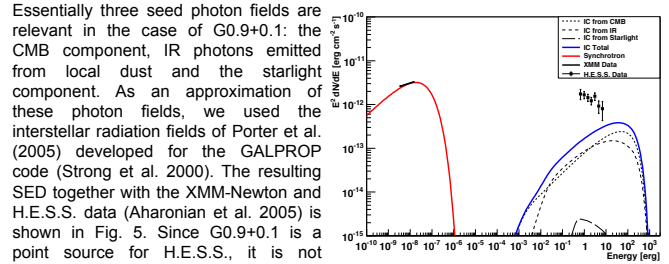


Fig. 5. SED of G0.9+0.1 showing the synchrotron and IC emission of the modeled area together with the XMM-Newton data of the modeled part as well as the H.E.S.S. data of the whole source (Aharonian et al. 2005).

Conclusion

We present an extensive analysis of the non-thermal X-ray emission of the PWN in the composite SNR G0.9+0.1. Furthermore we performed the first spatially resolved modeling of this source in the X-ray and VHE γ -ray energy range. For the modeling of the emission, we extracted spectra of annulus-shaped regions centered on the putative pulsar position. The evolution of the spectral index and surface brightness with increasing distance to the pulsar can be explained by assuming a leptonic outflow which suffers synchrotron and adiabatic energy losses as implemented in our model. We calculated the IC emission of the modeled part of the PWN using the parameters optimized to reproduce the X-ray emission. Particularly the unknown extent of G0.9+0.1 in that energy range impedes an appropriate comparison of the measured and modeled data. This problem may be solved with future Imaging Atmospheric Cherenkov Telescopes like the Cherenkov Telescope Array (CTA).

References

- Aharonian, F., Akhperjanian, A. G., Aye, K., et al. 2005, *A&A*, 432, L25
- Camilo, F., Ransom, S. M., Gaensler, B. M., & Lorimer, D. R. 2009, *ApJ*, 700, L34
- de Jager, O. C. & Harding, A. K. 1992, *ApJ*, 396, 161
- Gaensler, B. M., Pivovarov, M. J., & Garmire, G. P. 2001, *ApJ*, 556, L107
- Gaensler, B. M. & Slane, P. O. 2006, *ARA&A*, 44, 17
- Helfand, D. J. & Becker, R. H. 1987, *ApJ*, 314, 203
- Kennel, C. F. & Coroniti, F. V. 1984a, *ApJ*, 283, 694
- Kennel, C. F. & Coroniti, F. V. 1984b, *ApJ*, 283, 710
- Porquet, D., Decourchelle, A., & Warwick, R. S. 2003, *A&A*, 401, 197
- Porter, T. A. et al. 2005, in *International Cosmic Ray Conference*, Vol. 4, *International Cosmic Ray Conference*, 77
- Strong, A. W., Moskalenko, I. V., & Reimer, O. 2000, *ApJ*, 537
- Wilms, J., Allen, A., & McCray, R. 2000, *ApJ*, 542, 914



Bundesministerium
für Bildung
und Forschung